www.czasopisma.pan.pl PAN www.journals.pan.pl

ARCHIVES of FOUNDRY ENGINEERING

ISSN (2299-2944)
Volume 19
Issue 1/2019

89 – 97

DOI: 10.24425/afe.2018.125197

15/1

Published quarterly as the organ of the Foundry Commission of the Polish Academy of Sciences

The Influence of Solidification Rate on High-tin Bronze Microstructure

D. Bartocha *, C. Baron, J. Suchoń
Silesian University of Technology, Department of Foundry Engineering,
7 Towarowa Str. 44-100 Gliwice, Poland
* Corresponding author e-mail: dariusz.bartocha@polsl.pl

Received 10.12.2018; accepted in revised form 29.01.2019

Abstract

The most important feature of bells is their sound. Their clarity and beauty depend, first of all, on the bell's geometry - particularly the shape of its profile and the mechanical properties of alloy. Bells are the castings that work by emitting sound in as-cast state. Therefore all features that are created during melting, pouring, solidification and cooling processes will influence the bell's sound. The mechanical properties of bronze depend on the quality of alloy and microstructure which is created during solidification and depend on its kinetics. Hence, if the solidification parameters influence the alloy's properties, how could they influence the frequencies of bell`s tone? Taking into account alterable thickness of bell's wall and differences in microstructure, the alloy's properties in bell could be important. In the article authors present the investigations conducted to determine the influence of cooling kinetics on microstructure of bronze with 20 weight % tin contents.

Keywords: High-tin bronzes, Solidification rate, Microstructure, Bell's tone

1. Introduction

The struck bell can vibrates in a lot of modes, figures of vibrations, and in each mode with different frequency. The tone of bell's sound is depend on frequencies of that vibrations. The general pattern of mode frequencies is fixed by the so called profile [1]. For proper sound of bell the frequencies for the first few modes should be quite closely matched and be in the ratios 0.5 : 1.0 : 1.2 : 1.5 : 2.0... . That frequencies may be considered as a single notes consisting on bell tone, in that meaning are called partials. The firs one is called the hum, is not prominent, and the heard pitch is usually that of the second partial or 'prime', probably because it is reinforced by the harmonically-related partials with relative frequencies 2, 3 and 4. Because of the presence of the minor-third interval 1.2 in tone the minor chord (prime, minor-third and quint) exists, therefore the tone is perceived as complex.

The amplitude of the various partials in the sound of a bell could be affected by the a number of factors. These include:

- General mechanical characteristics of the bell, i.e. profile geometry, wall thickness and the composition of the alloy (mechanical properties),
- Mechanical properties of the clapper material and the dynamics of the impact as the clapper strikes the bell,
- The acoustic conditions in the building or space, where the bell is housed.

Besides it should be also aware that the perception of the of loudness of bell's sounds in the ear varies with frequency.

The natural frequencies of bell are the function of geometry (the shape of a profile) and mechanical properties of alloy in as-cast state, what describing equation (1). Therefore, in numerical

calculation i.e. modal analysis (natural frequencies determination) or designing (bell scaling, new shape of profile), the most important is validation of the model taking into account especial material properties. Especially because both the bell's geometry and the alloy microstructure thus its properties depend on molding, melting and casting processes.

$$([K] - \omega_i^2[M])\{\varphi_i\} = \{0\} \quad (1)$$

where:
[K] – stiffness matrix,
[M] – mass matrix,
ω - natural frequencies,
φ - mode shapes.

According to different sources, the value of Young's module for tin bronzes varies between 0.96 – 1.2E+5 MPa and density 7400 – 8900 kg/m^3 depending on the content of tin and other elements. The parameters of: melt process (time, temperature), liquid metal treatment (deoxidation, modification) [2-6] and solidification kinetics significantly influence the density of tin bronzes because of their tendency to porosity [2]. Hence such a large range of density values one can observe. Thus, the melting process and preparation of the metal can indirectly affect the tone of a bell [7]. Even taking into account single melt, while it could be assumed that: the chemical composition is constant and the parameters of melting process are also constant, variation of alloy's properties should be considered because the alloy's properties directly depends on solidification rate, that means the wall thickness and the bell size.

Assuming that the alloy's properties in-as cast state are the function of, first of all, its microstructure shaped during crystallization process and taking into account the differences in the wall thickness, it could be conclude that the properties depends on the wall thickness and are varied even in a single bell. Therefore it should be expected that the results of even well validated modelling are different than the values obtained from measuring.

Thus it seems to be possible to predict the alloy's properties on the base of chosen microstructure or crystallization parameters.

For the preparation of such inferencing, the cumulative analysis of data describing a crystallization process and microstructure as well as alloy's properties in quantitative way is essential.

2. Methodology

For the analysis of solidification and crystallization processes the Derivative Thermal Analysis (DTA) method was used. Investigation was carried with tester which had been worked out by authors, its geometry is presented in figure 1.a. A simplicity of tester geometry makes the limitation of model parts number possible, what translates into the ability to make it quickly and repeatable from various mold materials. Using the tester with equal wall thickness around the test casting and insulating its top surface with insulating lagging cause a one-direction, radius heat flow (fig. 1.b). Heat center of test casting coincides with its geometrical center, where a thermocouple type K (Ni-CrNi) was placed.

a)

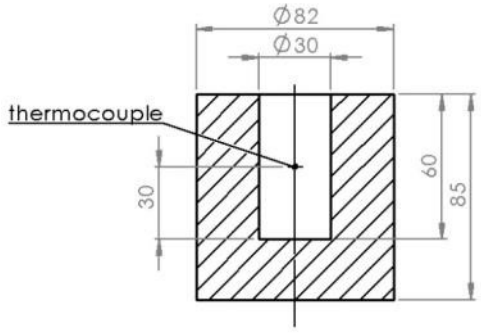

b)

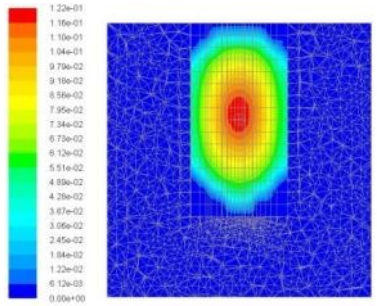

Fig. 1. a) Geometry of DTA tester, b) the example of the distribution of liquid phase fraction in the test casting during solidification – computer simulation

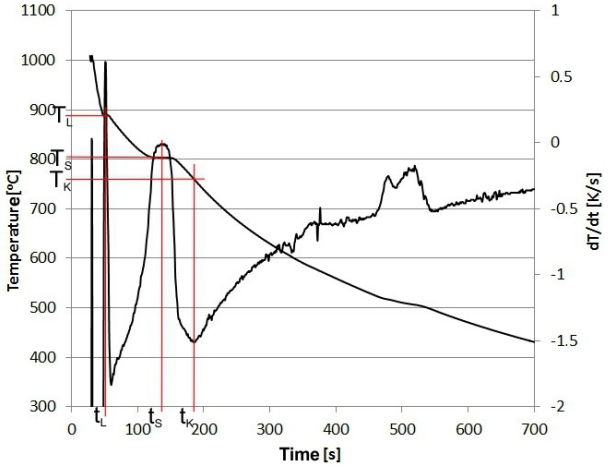

Fig. 2. Method of characteristic temperatures determination on the base of solidification and crystallization curves

On the base of solidification and crystallization curves analyzing the basic parameters describing solidification process of bronze CuSn20, such as liquidus temperature T_L, solidus temperature T_S, the end of crystallization temperature T_K (fig. 2.) as well as time of temperature decries in the ranges: $<T_L;T_S>$, $<T_L;T_K>$.

Test samples for microstructural investigations were cut from the center part of DTA casting, the place of cutting out the specimen is shown in figure 3.

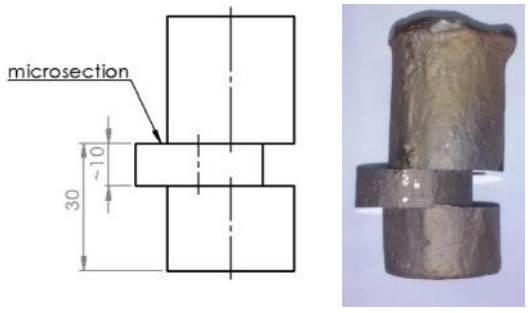

Fig. 3. The place of cutting out from DTA casting the specimen for microstructure investigations

Volumetric share of phase α and the average grain size of phase α are the microstructure stereological parameters that have been measured and determined. Measurement of these parameters were performed with automatic image analysis on the base of picture made on scanning microscope PhenomPro (fig. 4.a), while the analysis itself was carried out using software NIS-ELEMENTS BR 3.10. Moreover during the microstructure observation on scanning microscope, the tin concentration in each component of the microstructure were analyzed with EDS detector. The example of the measurement points arrangement is presented in figure 4.b.

a) b)

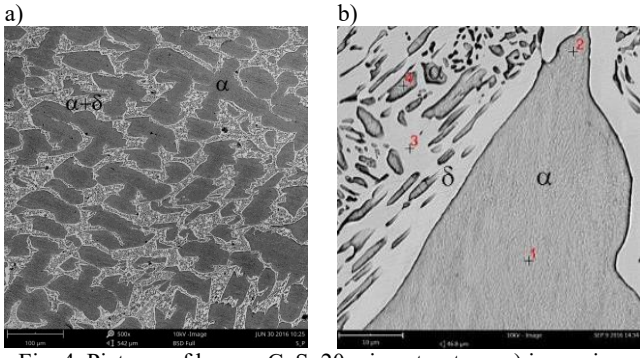

Fig. 4. Pictures of bronze CuSn20 microstructure: a) image in a format for quantitative analysis, b) the tin concentration measurement points arrangement 1- center, 2- grain's brink of primary phase α, 3- precipitates of phase δ and 4- precipitates of phase α in eutectoid mixture α+δ

3. Experiment

According to the plan of experiment five melts of CuSn20 alloy have been made, each melt was double, carried out twice, first time with pure tin and cooper as a charge materials (designation – C_20), second time by the remelting bronze CuSn20 (designation – S_20) obtained earlier.

As a part of each melts a test casting was made. Moulding materials, that were used for making the DTA tester mould, were selected, based on thermal properties (table 1). These materials should ensure significant differences in kinetics of test casting solidification and cooling, what is indicated by the values of thermal diffusivity "a". This coefficient indicates the material's susceptibility to temperature equalization during heating or cooling at specific locations. In a substance with high thermal diffusivity, heat moves rapidly through it because the substance conducts heat quickly relative to its volumetric heat capacity or 'thermal bulk' [8].

Table 1
Thermal properties of materials used to make test mould of

	density ρ [kg/m^3]	specific heat Cp [J/Kg K]	heat conductivity λ [W/m K]	thermal diffusivity a [m^2/s]**
Graphite [9, 10, 11, 12, 13]	1900	600-2150	135-12	$0.293 \cdot 10^{-6}$
OMF silica sand 20-1500°C [13, 14, 15, 16]	1550-1450	1021-1520	0.5-1.5	$0.068 \cdot 10^{-6}$
OMF silica sand + claydite 50/50 vol.	1225-975*	885-1385*	0.33-0.88*	$0.065 \cdot 10^{-6}$
Claydite (depending on the fraction) [17, 69, 19, 20, 21]	(900-500)	750-1250	0.16 – 0.26	$0.041 \cdot 10^{-6}$
Sibral 20-(700)-1500°C [13, 22]	430-380	590-(1200)-600	0.18-0.27	$0.059 \cdot 10^{-6}$
Traditional clay moulding sand [own inv.]	1550-1450	200-(350)-150	0.15-0.5	$0.099 \cdot 10^{-6}$

OMF – matrix of moulding sand, in each moulding sand as a binder the furane resin Kaltharz TDE 20 was applied,
* - values estimated on the base of sand and claydite properties,
** - values calculated ac. [9] for the values on right of presented ranges.

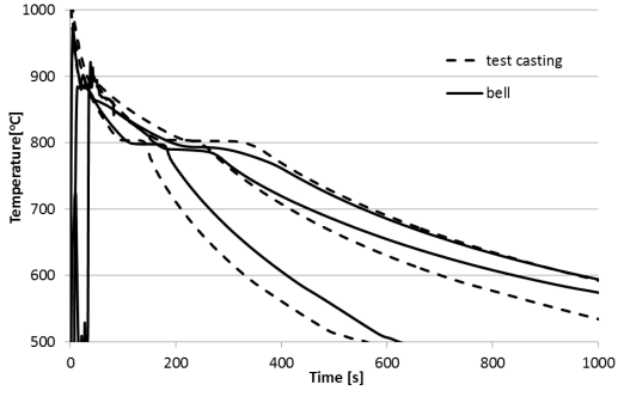

Fig. 5. Cooling curves of bronze CuSn20 recorded in testers made of: silica sand, silica sand + claydite and claydite moulding sand compared with curves recorded in the bell (weight circa 25kg) cast in mould made of traditional clay moulding sand

The application of three testers materials ensured the differentiation of cooling range similar to that one, which occurs in a small bell (fig. 5.). For the determination of wanted

dependence the two additional materials were applied: graphite and an aluminosilicate insulating material, its commercial name is Sibral. This made the range of cooling speed wider and should make it possible to find out if it ceases to play an important role after exceeding critical values.

Table 2.
Bronze's microstructure parameters

No	Mark	Tester material	vol. share. α %	average grain size α [μm²]	point 1 Sn wt. %	point 2 Sn wt. %	point 3 Sn wt.%	point 4 Sn wt. %
1	C_20	gr	52.57	396.95	18.5	18.1	33.8	21.8
2		p	56.84	2153.50	13.1	16.7	33.6	20.7
3		pk	59.87	1762.67	15.4	17.3	33.5	18.3
4		k	60.36	3612.13	16.9	18.6	33.5	19.8
5		s	53.72	3009.23	18.9	18.5	35.1	18.9
6	S_20	gr	55.92	446.42	14.34	19.44	31.8	19.98
7		p	57.94	2203.54	15.6	17.8	34.8	18.6
8		pk	60.08	3364.43	15.3	17.1	32.9	19.1
9		k	62.16	3943.45	17.1	17	33.5	20.8
10		s	55.37	3762.65	17.87	18.13	34.14	20.61

gr – graphite
p – silica sand
pk – silica sand + claydite
k – claydite
s – Sibral

4. Results

4.1 Microstructure

Microstructural investigations were carried out according to presented methodology, and the obtained results are presented in table 2. Pictures of bronze microstructures, from each melt, are shown in figure 7, moreover the graphical juxtaposition of results in the chart form is presented in figure 6.

4.2 Cooling kinetics

In the purpose of determination the basic parameters describing solidification process of test ingots, the analyze of cooling and crystallization curves was made. The obtained results are presented in table 3 as well as in graphical form as a charts in figures 8 – 9.

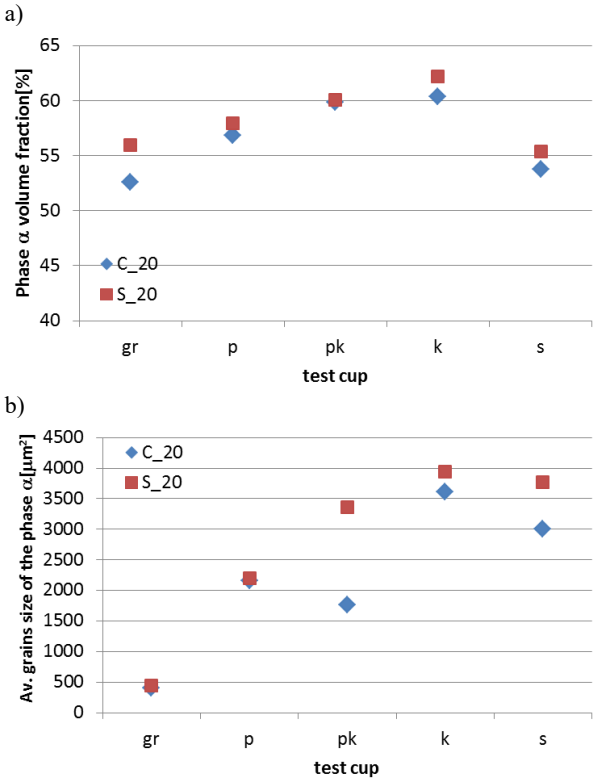

Fig. 6. Volume fraction a) and average grain size of phase α b), in dependence of tester material

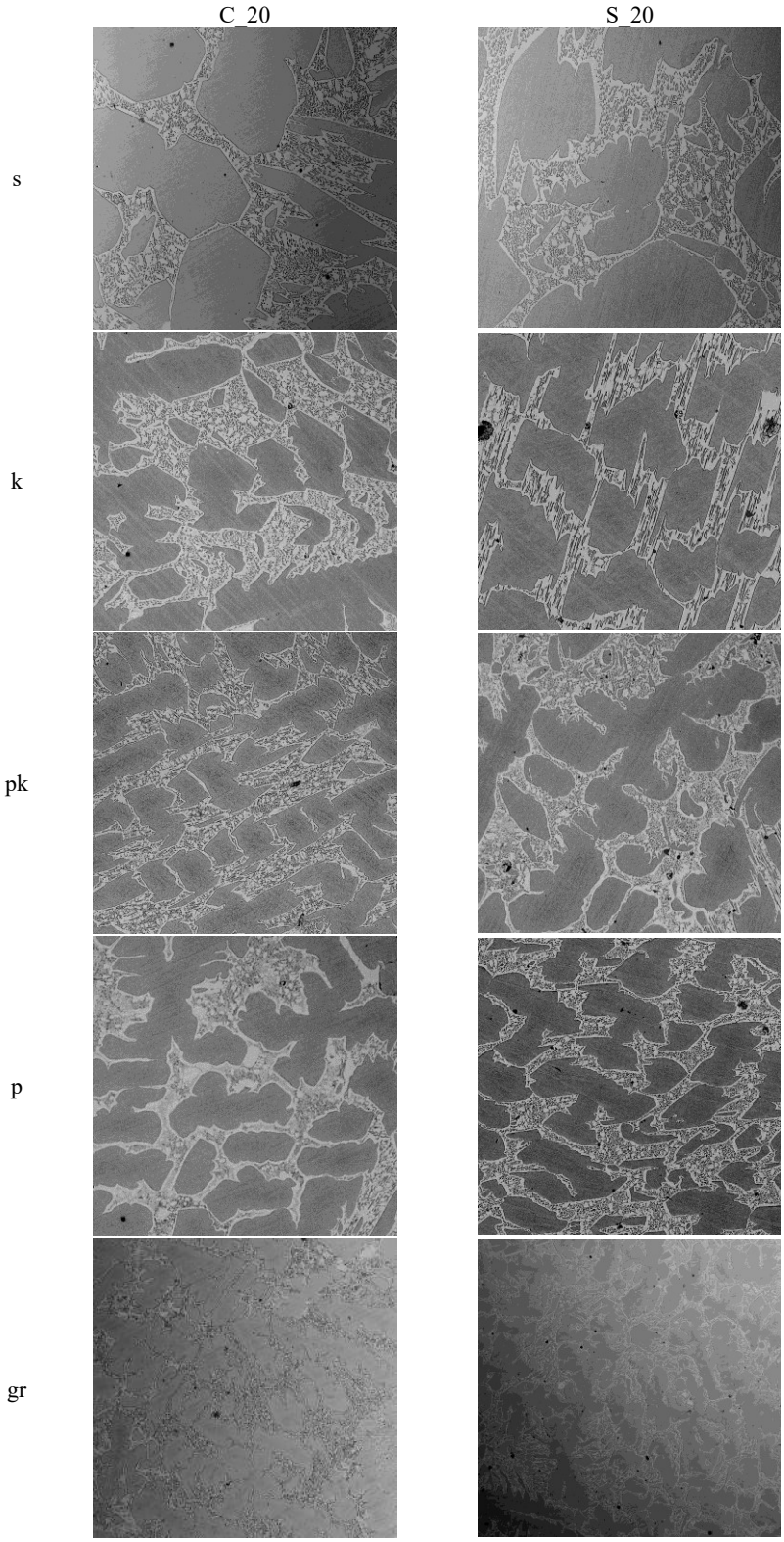

Fig. 7. Microstructure of bronze CuSn20, C_20 – melted from pure metal charge and S_20 – remelted, cast in tester made of; gr – graphite, p – silica sand moulding mix, pk – silica sand-claydite moulding mix, k – claydite moulding mix, s – sibral

Table 3.
Values of parameters describing solidification process of test ingots, determined on the basis of DTA curves analysis

No	Mark	Tester mat.	t_K-t_L [s]	t_S-t_L [s]	T_L [°C]	T_S [°C]	T_K [°C]	T_{max} [°C]
1	C_20	gr	11	7	888.7	814	774	897,4
2		p	122	80	886.3	803.5	787	995
3		pk	228	129	888.6	803.9	785.2	1006
4		k	330	178	889.9	802.7	781.1	1037
5		s	1358	828	896.4	806.9	785.7	1055
6	S_20	gr	11	6	890	819	764.9	967
7		p	148	96	894	801.7	779	1008
8		pk	177	107	893	802.6	779	999
9		k	382	210	891.8	800.6	780.9	1001
10		s	1345	790	896.8	804.3	782.3	961

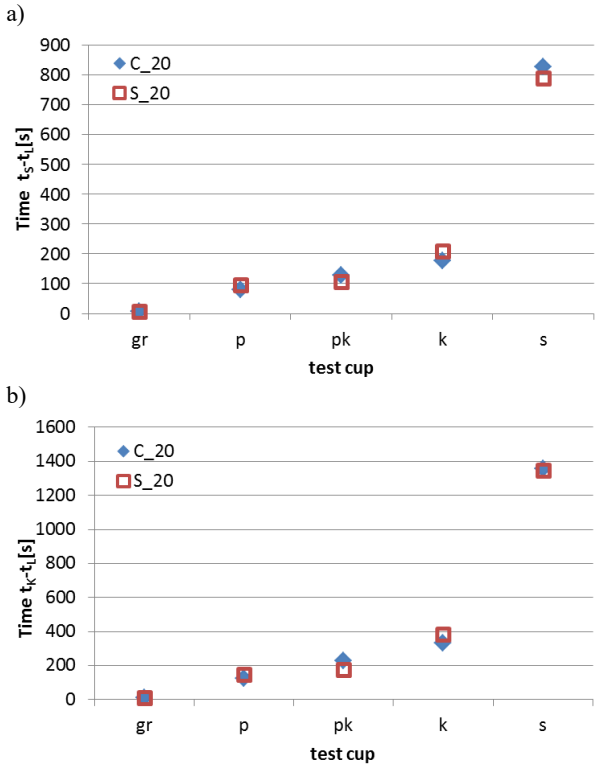

Fig. 8. Time of temperature decrease in the ranges a) <TL;TS> and b) <TL;TK>, in dependence of material of which tester have made

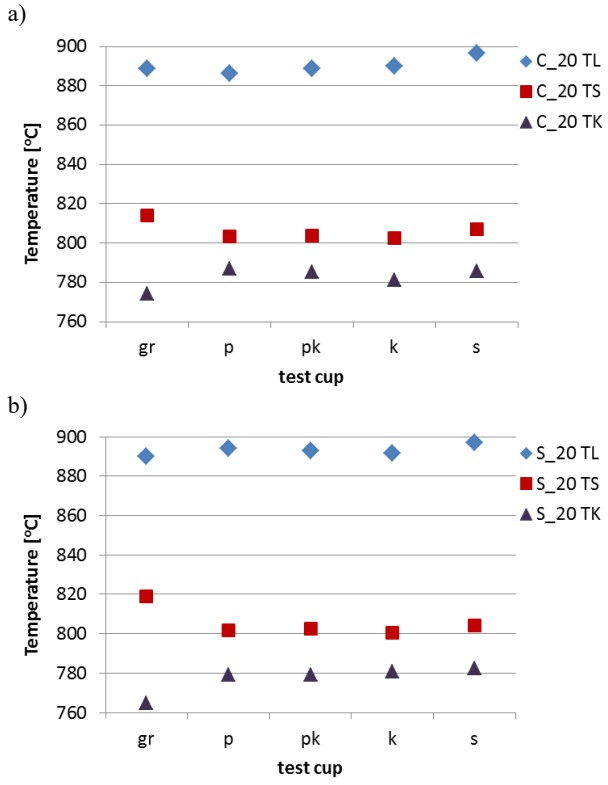

Fig. 9. Values of temperature T_L,T_S and T_K in dependence of material of which tester have made; a) bronze melted from pure metal charge C and b) remelted S

5. Discussion

According to the data available in literature [23 – 25] density of the phase α changes linearly from 8,96 to 9,04 [Mg/m3] in dependence of tin concentration <0 ; 9,28>, and the value of modulus of longitudinal elasticity changes also linearly from 124 to 113 [GPa] in similar tin concentration range. Density and value of Young's modulus of phase δ $Cu_{31}Sn_8$ (32,6% Sn) amount to accordingly 8,68 [Mg/m^3] and 80 [GPa]. Therefore, it should be presumed that the changes of bronze CuSn20's properties as an effect of different cooling speed during solidification are not the result of the quantitative changes triggered by that, but rather of the changes of properties of particular component of microstructure that are the effect of differences in speed of their crystallization.

By the analysis of the tin concentration changes in phase α dendrites, in the center of grain (measure point "1" fig. 4b) and on the grain's brink (measure point "2" fig. 4b), in the function of solidification time, a strong differentiations of tin concentrations in the solidification time range <0;200> s could be noticed, as well as in the center of grain and on the grain's brink. Moreover, with increasing solidification time above 200s, a stabilized value of tin concentration with a slight upward trend, with different intensity depending on a place of measure point is visible (fig. 10). Minimum of tin concentration value is moved in the direction of smaller solidification time in relation to maximum values of volumetric fraction and average grains size of phase α, and corresponds with cooling speeds obtained in tester made of silica sand. The value of tin concentration in phase α measured in bronze cast in graphite tester, the smallest solidification time due to very large grain fragmentation and size of the EDS head detection area and, what is connected with this, a high probability of influence the other microstructure components on the measurement result, should be considered as a value loaded by too big error.

Short time of solidification, an actually high speed of crystallization causes decreasing amount of phase α in the bronze microstructure, what should cause decreasing of modulus of longitudinal elasticity and density as well as increasing value of Poisson ratio. But in the same time, because of crystallization kinetic limits solubility of tin in Cu-Sn solution, the lines on equilibrium chart are moved towards the lower tin content (fig. 11), and a decrease in tin content in the phase α results in a significant increase in its Young's modulus and a slight decrease in density [23 – 25].

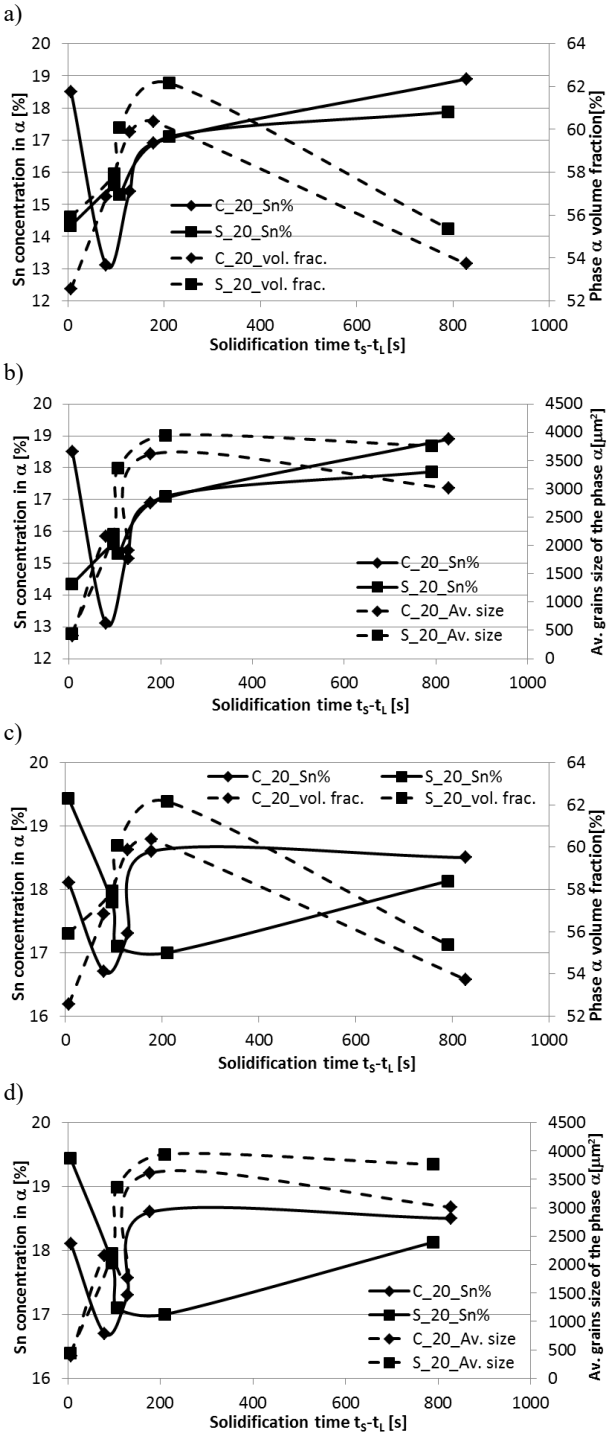

Fig. 10. Changes of tin bronze microstructure parameters and tin concentration in phase α in dependence of solidification time; a) and b) concentration measured in point „1" (fig. 4b); c) and d) concentration measured in point „2" (fig. 4b)

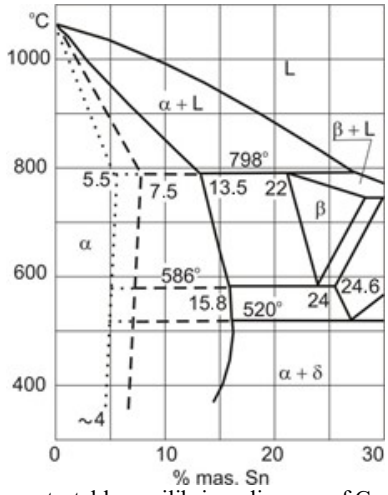

Fig. 11. The metastable equilibrium diagram of Cu-Sn; dashed line – casting solidifying in sand mould , dotted line – casting solidifying in permanent (metal) mould [26]

Whether? The increasing of Young's moduli as an effect of decreasing tin content in phase α is such big that compensates, with extra amount, expected decreasing of Young's moduli value of bronze as a result of decreasing of phase α amount in its structure. It should be remembered that the solidification rate influences the microstructure fine-grained The higher solidification speed causes significant fragmentation of bronze structure and as a result the simultaneous increase in the properties of bronze.

Decreasing of phase α amount and tin concentration in it should effect in decreasing of bronze density. But shorter solidification time and hence higher solidification rate and temperature gradient promote the directional solidification, what in turn prevent to create the interdendritic micro-pores (empties), such characteristically for the microstructure of bronzes solidifying with lower speed.

The above analysis shows that properties of bronze CuSn20 depend on values of quantitative parameters, morphology, chemical contents and properties of its microstructure components, while those are the effects of the crystallization process course, first of all peritectic reaction and transformation.

6. Conclusions

It emerges from the above discussion that, irrespective to the type of factor determining the morphology and the amount of components of the bronze microstructure, its properties are strictly and univocally related to it.

It is obvious that knowing quantitative relationships between microstructure parameters and mechanical properties allows us to determine the bronze's properties on the basis of values of parameters describing its microstructure.

Going a step further and describing in a quantitative manner the dependence of the bronze structure on the parameters of the crystallization process that determine it, the selected properties of the bronze based on the values of the crystallization parameters could be directly determined.

To determine the distribution of the properties of bronze, for example in a bell, it is necessary to provide data on the values and differentiation of solidification times in the region of casting part. The values of solidification time, practically for any castings point, can be determined based on computer simulations of the process of its solidification and cooling, with correct, validated, thermo-physical properties of bronze.

References

[1] Fletcher, N.H., (1999) *The nonlinear physics of musical instruments*. Reports on Progress in Physics. 62, 723-764.
[2] Bartocha, D. & Baron, C. (2015). „The Secret" of Traditional Technology of Casting Bells. *Archives of Foundry Engineering.* 15(spec.3), 5-10. (in Polish).
[3] Czochlarski, J. & Bukowski, Z. (1935). Deoxidation of brasses and bronzes. Warszawa: Wiadomości Instytutu Metalurgii.
[4] Bydałek, A.W. (2009). The analysis of carbon attendance in copper alloys as reason of gas porosity. *Archives of Foundry Engineering.* 9(3), 25-28.
[5] Bydałek, A.W. (1999). Melting of chosen cooper alloys in reducing conditions. *Solidification of Metals and Alloys.* 1(40), 87-92. (in Polish).
[6] Bydałek, A.W. (2005). Analysis of cooper alloys melting technology on castings porosity. *Archives of Foundry.* 5(17), 27-36, (in Polish).
[7] Bartocha, D. & Baron, C. (2016). Influence of Tin Bronze Melting and Pouring Parameters on Its Properties and Bells' Tone. *Archives of Foundry Engineering.* 16(4), 17-22.
[8] Wiśniewski, S., Wiśniewski, T.S. (1994). *Heat exchange*. Warszawa: Wydawnictwo Naukowo-Techniczne. (in Polish).
[9] Janerka, K. (2013). *The influence of carburizers on the microstructure and properties of cast iron.* Katowice-Gliwice: Wydawnictwo Archives of Foundry Engineering. (in Polish).
[10] Bartocha, D. & Janerka, K. (2010). Carburizer particle dissolution in liquid cast iron – computer simulation. *Archives of Foundry Engineering.* 10(1), 7-14.
[11] Janerka, K. & Bartocha, D. (2010). Computer simulation of carburizers particles heating in liquid metal. *Archives of Foundry Engineering.* 10(1), 59-67.
[12] Taler, J., Duda, P. (2003). *Solving the simple and inverse issues of heat transfer*. Warszawa: WNT (in Polish).
[13] NovaFlow&Solid CV4.4r3 software material data base.
[14] Ignaszak, Z. (1999). Simulation model sensitivity to quality of material properties. *Solidification of Metals and Alloys.* 1(40), 25-36.
[15] Ignaszak, Z. (2002). *Virtual prototyping in foundry. Data Bases and validation*. Poznań: Wydawnictwo Politechniki Poznańskiej. (in Polish).
[16] Ignaszak, Z. & Prunier, J-B. (2017). Innovative Laboratory Procedure to Estimate Thermophysical Parameters of Iso-exo Sleeves. *Archives of Foundry Engineering.* 17(1), 67-72.
[17] Gernot Minke (2007). Building with Earth: *Design and Technology of a Sustainable Architecture. Birkhäuser Basel*.

[18] Sailor, D.J. & Hagos, M. (2011). An updated and expanded set of thermal property data for green roof growing media. *Energy and Buildings.* 43, 2298-2303.
[19] Davraz, M., Koru, M. & Akdağ, A.E. (2015). The Effect of Physical Properties on Thermal Conductivity of Lightweight Aggregate. *Procedia Earth and Planetary Science.* 15, 85-92.
[20] Franus, M. (2012). Physical and mechanical properties of expanded clay obtained with the addition of glauconite. *Budownictwo i Architektura.* 10, 5-14. (in Polish).
[21] List of physical parameters of materials and construction products. acc. PN-EN ISO 12524:2003, PN-EN ISO 6946:1999 i PN-91/B-02020.
[22] Data sheet: AWOTEX-2 FIBERFRAX – SIBRAL.
[23] Perrin, R., Swallowe, G.M., Charnley, T. & Marshall, C. (1999). On the debossing, annealing and mounting of bells. *Journal of Sound and Vibration.* 227(2), 409-425.
[24] Fields R., Low S. & Lucey G. (1991). Physical and mechanical properties of intermetallic compounds commonly found in solder joints. *Metal Science of Joining, Cincinnati.* Oct 20-24.
[25] Subrahmanyam, B. (1972). Elastic Moduli of some complicated binary alloy systems. *Transactions of Japan Institute of Metals.* 13, 93-95.
[26] Górny, Z. (1992). *Non-ferrous foundry alloys*. Warszawa: WNT. (in Polish).